ORIGINAL ARTICLE

Synthesis of chitosan-stabilized copper nanoparticles (CS-Cu NPs): Its catalytic activity for C-N and C-O cross-coupling reactions and treatment of bladder cancer

Zhou Hongfeng [a], Attalla El-Kott [b,c], Ahmed Ezzat Ahmed [b,d], Ahmed Khames [e]

[a] Deparment of the Seventh Department of Medical Oncology, Harbin Medical University Cancer Hospital, Harbin 150081, China
[b] Biology Department, College of Science, King Khalid University, Abha, Saudi Arabia
[c] Zoology Department, Faculty of Science, Damanhour University, Damanhour, Egypt
[d] Theriogenology Department, Faculty of Veterinary Medicine, South Valley University, qena, 83523 Qena, Egypt
[e] Department of Pharmaceutics and Industrial Pharmacy, College of Pharmacy, Taif University, P.O. Box 11099, Taif 21944, Saudi Arabia

Abstract Herein, we report the synthesis of copper nanoparticles at ambient conditions using biopolymer, chitosan, as a protecting and stabilizing agent and hydrazine as a reducing agent. The obtained nanoparticles (CS-Cu NPs) were characterized using XRD, FT-IR, FE-SEM, EDS, TEM and UV–Vis spectroscopy. This nanocomposite was utilized as an efficient heterogeneous nanocatalyst for the aryl and heteroaryl C–N and C–O cross coupling reactions with excellent yields at mild conditions. The nanocatalyst were isolated and reused for 10 times with reproducible catalytic activity. Cell viability of nanocomposite was very low against bladder cancer (UM-UC-3 (Transitional cell carcinoma), SCaBER (Squamous cell carcinoma), and TCCSUP (Grade IV, transitional cell carcinoma)) cell lines without any cytotoxicity on the normal cell line. The best anti-human bladder cancer properties of nanocomposite against the above cell lines was in the case of TCCSUP cell line. According to the above findings, the nanocomposite may be administrated for the treatment of several types of human bladder cancer in humans.
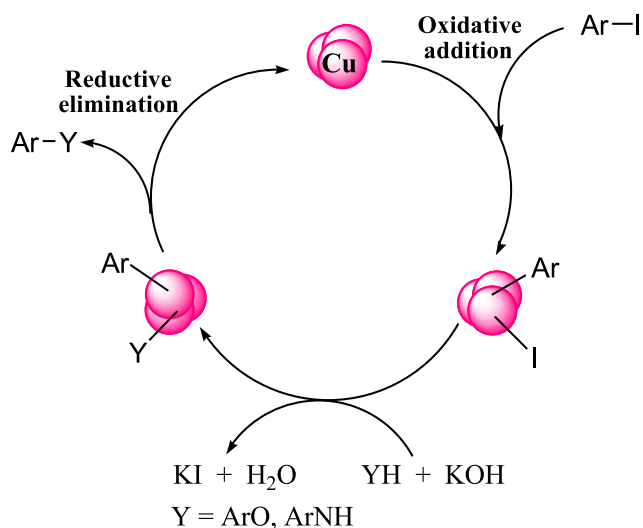© 2021 Published by Elsevier B.V. on behalf of King Saud University. This is an open access article under the CC BY-NC-ND license (http://creativecommons.org/licenses/by-nc-nd/4.0/).

1. Introduction

In the last few years the C-C, C-N and C-O cross-coupling reactions have garnered significant impetus since they construct the backbone of copious pharmacophores and naturally occurring biologically potent molecules (Craig, 1991;

Yoshikawa et al., 1998; Nair et al., 2004,2002; Stabler, 1994). Hence, the organic researchers around the world have engaged them in persistent hunt towards the facile and proficient synthetic methodologies of these compounds. Among all, the catalyzed heteronuclear C-N/O coupling seems to be the most simplified and competent pathway. In so doing, several catalytic systems based on noble metal catalysts, particularly with Pd, Ag and Au, have been reported (Hartwig, 2000; Hartwig, 1998; Rodriguez et al., 2020; Akram et al., 2019; Capdevila et al., 2018; Das et al., 2013). However, expensiveness of the starting materials in the synthesis of novel catalysts and also their respective stability has been a constraint in their use. In this regard, Cu has come up with its unique features like its abundance, being economical, eco-friendly, stable and also a promising candidate to carry out such coupling reactions (Kuo and Huang, 2010; Zhang et al., 2014; Xu et al., 2016; Ranu et al., 2012; Ranu et al., 2013; Sambiagio et al., 2014; Son et al., 2004; Rout et al., 2007; Kidwai et al., 2010; Pai and Chattopadhyay, 2014; Reddy et al., 2015; Nador et al., 2014; Mitrofanov et al., 2017; Halder et al., 2017).

Chitosan is an interesting biopolymer which is obtained from the fishery wastes or *N*-deacetylation of chitin in alkaline media (Makhubela et al., 2011). Its low cost, abundance, hydrophilicity, biodegradability and significant thermal stability has grabbed profound attention (Leonhardt et al., 2010; Muzzarelli, 2011; Adlim et al., 2004). In addition, they have interesting functionalities like –NH2 and –OH groups which provides a suitable arrangement like a chelating ligand to coordinate different metal ions (Xu et al., 2010; Guinesi and Cavalheiro, 2006). There are several reports on catalytic applications of metal chelated chitosan (Zhu et al., 2012; Baran et al., 2015; Baran and Menteş, 2015; Antony et al., 2013).

Based on applicative engineered nanomaterials, we are prompted to synthesize an CS-Cu NPs nanocomposite by adorning Cu NPs over the chitosan polysaccharide. In this method, the chitosan biopolymer, acts as capping and stabilizing agent and hydrazine as a reducing agent. Next, we describe its excellent catalytic activity for the synthesis of C–N and C–O cross coupled products (Scheme 1). We also investigated the prepared nanocomposite in the cytotoxicity studies against common human bladder cancer cell lines i.e., UM-UC-3 (Transitional cell carcinoma), SCaBER (Squamous cell carcinoma), and TCCSUP (Grade IV, transitional cell carcinoma) cell lines, *in-vitro*. Interestingly, we got significantly good results in the study. The best result was achieved in case of TCCSUP cell line Scheme 2.

2. Experimental

2.1. Synthesis of chitosan-stabilized copper NPs (CS-Cu NPs)

In a typical experiment, 200 mL of 1% water-soluble chitosan solution was added to 50 mL of distilled water containing 20 mg of $CuCl_2$ to make a reaction mixture through vigorous stirring. The pH of the solution was adjusted to basic (pH = 9) using 200 µL of concentrated ammonia solution. The reaction was allowed to proceed under gentle stirring at room temperature for 10 min. The color changes from greenish blue to blue due to the formation of copper-ammonia complex. After 10 min of gentle mixing, 500 µL of hydrazine hydrate was added as a mild reducing agent. After stirring the solution for 5 min, the reaction was allowed to proceed at room temperature for 5 hrs. The formation of copper nanoparticles was easily noticeable due to the change in the color of the solution to reddish brown – the characteristic color of the copper nanoparticles (Cu NPs). The CS-Cu NPs were powdered by the freeze-drying mechanism.

Scheme 1   Schematic preparation of chitosan-stabilized copper nanoparticles and its catalytic activity for C–N and C–O cross coupling reactions.

Scheme 2 Possible reaction pathway for CS-Cu NPs catalyzed C-N and C-O bonds formation.

2.2. General procedure for C-N and C-O cross-coupling reactions catalyzed over CS-Cu NPs

A mixture of N/O nucleophile (1 mol%), aryl halide (1 mol%) and KOH (1 mol%) and aqueous chitosan stabilized Cu NPs (0.2 mol %) were suspended in 3 mL DMSO. The resulting mixture was heated at 100 °C under N_2 atmosphere with stirring until the reaction was complete as judged by TLC (ethyl acetate/hexane; 1/5). On completion, the catalyst was recovered by centrifugation and washed with water and dried at 60 °C for reuse. The filtrated phase was diluted with ether, washed with brine and dried over magnesium sulfate. The related products were purified by silica gel flash chromatography using EtOAc and hexane as eluent. The related products were characterized by ^1H NMR and ^{13}C NMR analysis.

2.3. Determination of anti-human bladder cancer effects of nanocatalyst

In this assay, different human bladder cancer cell lines i.e., UM-UC-3 (Transitional cell carcinoma), SCaBER (Squamous cell carcinoma), and TCCSUP (Grade IV, transitional cell carcinoma) cell lines and also the normal cell line (HUVEC) were used to study the cytotoxicity and anticancer potential of human bladder over the CS-Cu NPs using the common cytotoxicity test i.e., MTT assay *in vitro* condition. For culturing the above cells, several materials including penicillin, streptomycin, and Dulbecco's modified Eagle's medium (DMEM) were used (Zangeneh et al., 20192019201920202020). The distribution of cells was 10,000 cells/well in 96-well plates. All samples were transferred to a humidified incubator containing 5% CO_2 at 37 °C. After 24 h incubation, all cells were treated with the different CS-Cu NPs samples (0–1000 μg/mL) and incubated again for 24 h. Subsequently, they were sterilized by UV-radiation for 2 h. Then 5 mg/mL of MTT was added to all wells and were incubated again for 4 h at 37 °C. The percentage of cell viability of samples were determined following the given formula after the measurement of absorbance at 570 nm.

$$Cellviability(\%) = \frac{SampleA.}{ControlA.} x100$$

2.4. Qualitative measurement

The obtained results were loaded into the "SPSS-22" program and evaluated by "one-way ANOVA", accompanied by a "Duncan post-hoc" check ($p \leq 0.01$).

3. Results and discussion

The chemical reduction of metal salt is one of the most convenient and promising synthetic method to obtain metal NPs with relatively inexpensive procedures. Copper nanoparticles are very difficult to make by simple reduction of copper salts in aqueous solution, when compared with other metals such as Au, Ag, or Pt, since copper oxidizes to CuO and Cu_2O (Mallick et al., 2012; Mallick et al., 2006; Zain et al., 2014). However, the pure synthesis of Cu NPs can be obtained by using a carrier material, such as a polymer matrix e.g., chitosan which is having a good copper binding properties (Zain et al., 2014; Cardenas et al., 2002). This polymer has been used as a reducing agent and capping agent in the synthesis of Cu NPs, which avoid its aggregation and oxidation reaction. Here in this investigation, we described a simple synthesis of Cu NPs via a chemical method under an ambient atmosphere with chitosan (CS) as stabilizer-capping and hydrazine as the reducing agent. The as synthesized CS-Cu NPs are thoroughly characterized by different physicochemical techniques like Fourier Transformed Infra-Red (FT-IR), Field Emission Scanning Electron Microscopy (FESEM), Energy Dispersive X-ray Spectroscopy (EDX), Transmission Electron Microscopy (TEM), UV–Vis spectroscopy, and X-ray diffraction (XRD).

The FT-IR analysis was performed to identify the molecular interactions between the CS and the synthesized Cu NPs (Fig. 1). In the FT-IR spectra of chitosan (Fig. 1a) the broad peak appeared at 3401 cm^{-1} corresponds to the overlapped stretching vibrations of NH_2 and OH groups (Chen and Wu, 2000). The alcoholic C–O stretching, C–N stretching and N–H bending peaks are observed at 1013 cm^{-1}, 1369 cm^{-1} and 1570 cm^{-1} respectively (Dang and Le, 2011). A similar trend was observed in the CS mediated Cu NPs spectrum (Fig. 1b). For instance, a general decrease in band with a blue shift was noticed (from 3401 to 3382, 1570 to 1575, 1369 to 1346 and 1013 to 1005 cm^{-1}) (Chen and Wu, 2000). However, a new absorption peak was observed at 461 cm^{-1}. The corresponding vibration band is related to the interaction between the Cu NPs and the CS media, which indicates a reaction between the Cu NPs surface, and the CS amino and hydroxyl groups. This suggests that NPs were capped by the polymer (Raffi et al., 2010).

The FE-SEM image presented in Fig. 2a indicates the defined spherical morphology of the prepared Cu NPs. All Cu NPs have the mean particles size of nanometer. It is observed that the prepared Cu NPs results comparably small spherical particles with uniform dimension. The TEM images provide detailed morphological insights on the shape and dimension of these Cu NPs. As the images shown in Fig. 2b, the Cu NPs are being synthesized with moderately good monodispersity and almost spherical structures ranging from 10 to 20 nm with no agglomeration.
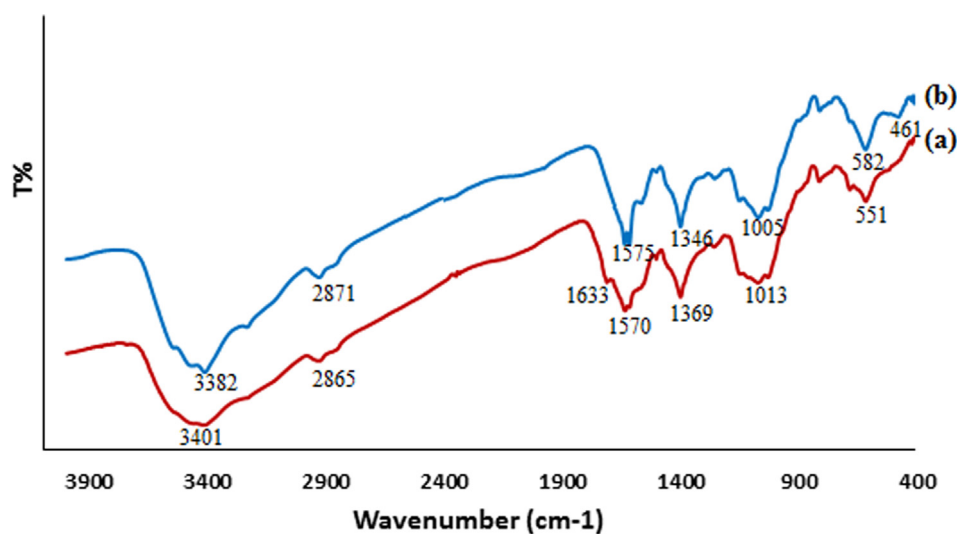
Fig. 1   FT-IR spectrum of (a) CS and (b) CS-Cu NPs.
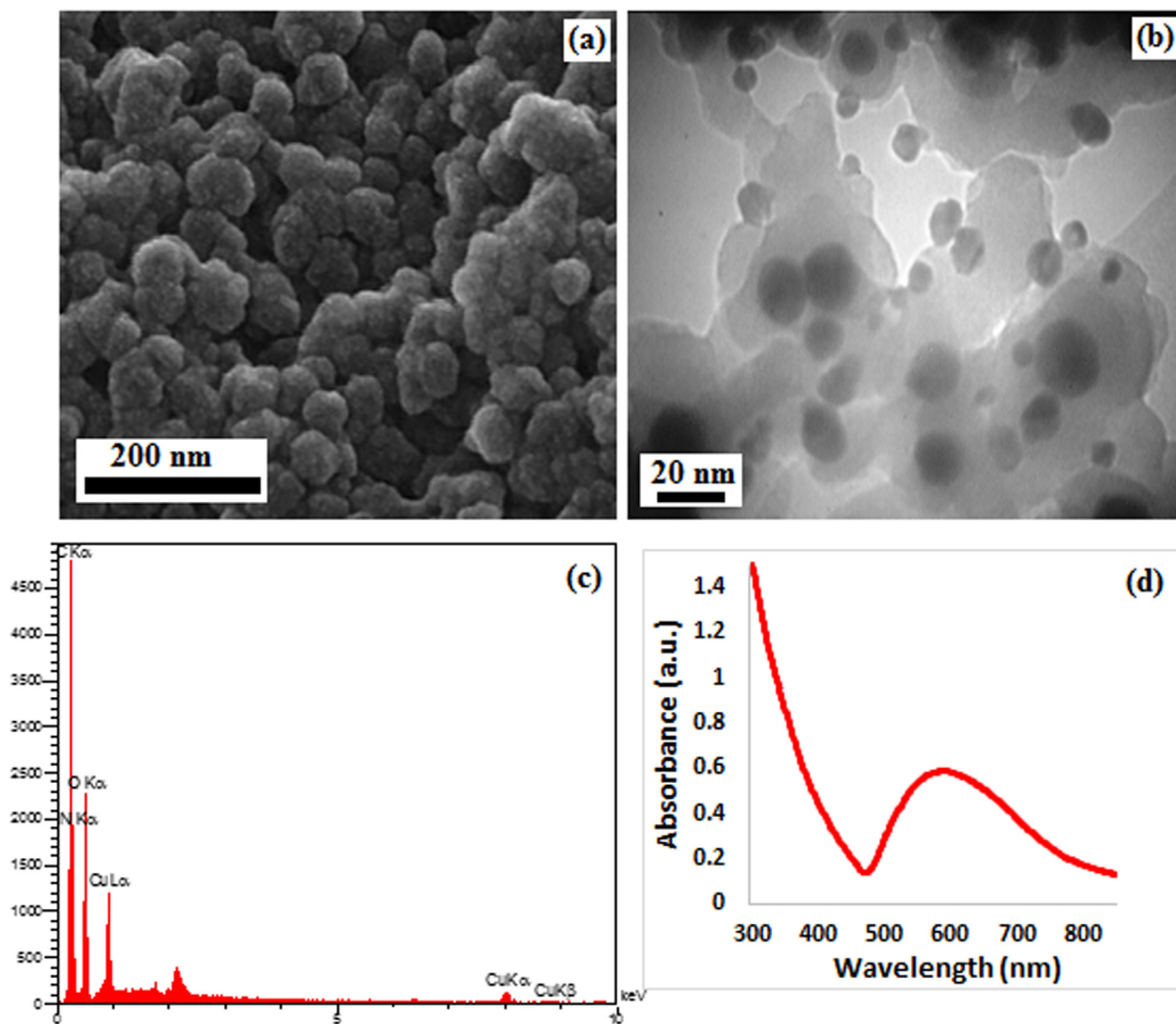

Fig. 2   (a) FESEM, (b) TEM images of CS-Cu NPs with (c) its EDX pattern and (d) UV–Vis spectrum.

The composition of synthesized Cu NPs has been studied through EDX analysis, as observed in Fig. 2c. The spectrum shows C, N, Cu and O peaks. The presence of nitrogen demonstrates the presence of chitosan that bonded to the Cu NPs. UV–Vis spectroscopy is a potential measure for the identification of Cu NPs. The spectrum recorded at different time intervals of the reaction are presented in Fig. 2d. After 5 h, the reaction was ended with the formation of Cu NPs which was confirmed by the characteristic surface plasmon absorbance (sky blue line) at 588 nm. Variations in color of the reaction aliquots indicated the gradual reduction of Cu^{2+} salt to Cu^0 NPs (Xie et al., 2006).

Crystallinity of the prepared Cu NPs was ascertained by XRD analysis (Fig. 3). The selected sample of copper nanoparticles shows a structure characterized by peaks at 2θ: 43.2 (1 1 1), 50.3 (2 0 0), and 74.1 (2 2 0), which match exactly with the standard data of Cu crystals from Joint Committee on Powder Diffraction Standards (JCPDS No.04–0784).

Once having the structural affirmation of synthesized CS-Cu NPs by rigorous instrumentation, the catalytic performance of these NPs was assessed in the carbon-heteroatom cross coupling reactions. In order to optimize the reaction conditions, a series of experiment was carried out with the variation of different reaction parameters like catalyst load, base, solvent and temperature over a model reaction of iodobenzene with indole and phenol. The results have been documented in Table 1. While carrying out the C-N coupling reactions of indole, it failed in the absence of catalyst and the additive base (Table 1, entry 9, 10) indicating their importance. Among the different bases used, KOH was found to be most effective resulting highest yield at 100 °C (Table 1, entry 8). We also screened the reaction in different solvents like EtOH, toluene, DMF, DMSO, CH_2Cl_2, CH_3CN (entry 1–8). Interestingly, DMSO resulted the best yield in shortest reaction time. It was also observed that 0.2 mol% catalyst loads were optimum to have the best catalytic results (Table 1, entry 8). We examined the reaction at different temperature too. However, at lower conditions it was not much successful and we continued at 100 °C (Table 1, entry 15, 16). After the fruitful experimentation for the best reaction conditions with N nucleophile (indole), we continued the same with O nucleophile like (phenol) and got delighted to have excellent result with this even in shorter reaction time (Table 1, entry 21). Therefore, the results revealed the optimized conditions for the reaction of N/O

nucleophiles (1.0 mmol) with iodobenzene (1.1 mmol) using 1.5 mmol KOH in DMSO at 100 °C over 0.2 mol% CS-Cu NPs as catalyst.

On stabilizing the reaction conditions as discussed in Table 1, it was the turn to prove the generality of them over a wide range of N- and O-nucleophiles reacting with diverse aryl iodides to furnish a library of C-heteroatom cross coupled products (Table 2). Different aryl and heteroaryl N-nucleophiles like indole, imidazole and aniline reacted at high compatibility with wide range of electron withdrawing and electron donating functional group substituted (Cl, CH_3, OCH_3, NO_2 etc) aryl iodides affording good to excellent yields (Table 2, entry 1–15). Notably, aniline reacted with the aryl iodides at a faster rate than indole or imidazoles (Table 2, entry 7–12). The same reaction trend is followed with O-nucleophiles like substituted phenol derivatives with different aryl iodides. Interestingly, here also the corresponding nucleophiles reacted outstandingly producing high yields in short reaction times irrespective of the substitutions. All the products were known and further confirmed by spectroscopic studies.

In view of industrial application, the test of reusability of the catalyst is an imperative aspect. Thereby, the reaction of indole and iodobenzene was chosen as a model reaction with a larger batch size (2.0 mmol) under optimized conditions. After complete reaction the catalyst was separated by centrifugation, washed with ethanol, dried and reused in the next run. Interestingly, we could use it for 10 successive runs without discernible change in catalytic activity (Fig. 4). The catalyst was robust enough and no leaching was found determined by ICP-OES analysis of the catalyst after 10th run.

To determine the heterogeneity of the catalyst, a hot filtration test was performed for the same above reaction. After a half long pathway of the reaction the catalyst was isolated from the reaction mixture by filtration and continued further. Significantly, there was no further increase in the yield, verifying heterogeneity of the catalyst. The XRD analysis (Fig. 5) of the reused catalyst after 10th cycles confirmed the protection and stability of the catalyst's nanostructure.

While concerning about the mechanism it is believed that the reaction goes through oxidative addition followed by reductive elimination pathway. At the outset, aryl iodide molecule binds to the surface of Cu NPs. At intermediate stage, the nucleophile reacts in the presence of KOH to generate the potassium salt of them which further substitutes the halide ion bonded to catalyst surface. The aryl group and nucleophile finally adds up over the catalyst and gets eliminated as coupled product leaving behind the active catalyst (Ranu et al., 2013).

The higher free radical concentration in the normal cells causes mutation of DNA and RNA structure, breaks down their gene expressions, which helps to accelerate the proliferation and growth of abnormal or cancerous cells. The elevated free radical density in different cancers cells points out their significant roles towards angiogenesis and tumorigenesis (Zangeneh et al., 2019). The anticancer potential of therapeutic compounds against human bladder cancer cell lines is immensely related to their antioxidant properties. Several earlier reports have uncovered that therapeutic compounds with strong antioxidant capacity significantly inhibits the growth of cancer cells by removing free radicals (Zangeneh et al., 2019). This is our earnest effort in exploiting nanocatalyst towards the adenocarcinoma studies and the corresponding
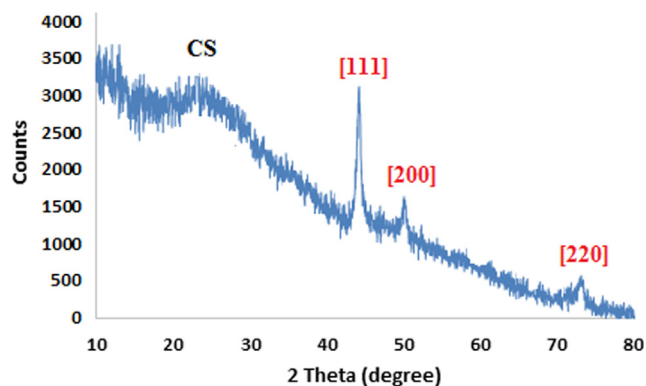

Fig. 3 Powder XRD pattern of CS-Cu NPs.

Table 1 Optimization of reaction condition for CS-Cu NPs-catalyzed coupling of indole/phenol with iodobenzene.[a]

NuH + [iodobenzene structure] ⟶ [phenyl-Nu structure]

Entry	NuH	Cat. (mol%)	Base	Solvent	T (°C)	t (h)	Yield(%)[b]
1	Indole	0.1	KOH	EtOH	100	10	60
2	Indole	0.1	KOH	DMSO	100	8	75
3	Indole	0.1	KOH	Toluene	100	10	70
4	Indole	0.1	KOH	DMF	100	10	70
5	Indole	0.1	KOH	CH_2Cl_2	100	24	40
6	Indole	0.1	KOH	CH_3CN	100	24	50
7	Indole	0.15	KOH	DMSO	100	8	85
8	**Indole**	**0.2**	**KOH**	**DMSO**	**100**	**8**	**96**
9	Indole	0.2	–	DMSO	100	24	Trace
10	Indole	–	KOH	DMSO	100	24	0
11	Indole	0.2	K_2CO_3	DMSO	100	8	70
12	Indole	0.2	Na_2CO_3	DMSO	100	8	65
13	Indole	0.2	Et_3N	DMSO	100	8	70
14	Indole	0.2	$NaHCO_3$	DMSO	100	8	60
15	Indole	0.2	KOH	DMSO	80	8	60
16	Indole	0.2	KOH	DMSO	25	8	30
17	Phenol	0.2	KOH	EtOH	100	12	35
18	Phenol	0.2	KOH	Toluene	100	8	55
19	Phenol	0.2	KOH	DMF	100	8	85
20	Phenol	0.2	KOH	CH_3CN	100	7	70
21	**Phenol**	**0.2**	**K_2CO_3**	**DMSO**	**100**	**7**	**90**
22	Phenol	0.2	Et_3N	DMSO	100	7	80
23	Phenol	0.2	K_2CO_3	DMSO	25	12	30
24	Phenol	0.1	K_2CO_3	DMSO	100	12	70
25	Phenol	0.3	K_2CO_3	DMSO	100	7	90

[a] Reaction conditions: N/O nucleophile (1.0 mmol), iodobenzene (1.1 mmol), CS-Cu NPs, base (1.5 mmol), solvent (3.0 mL), N_2 atmosphere; [b]Isolated yield.

Table 2 CS-Cu NPs-catalyzed coupling of amines and phenols with aryl iodides.[a]

Entry	Substrate	Aryl Iodide	Time (h)	Yield (%)	Ref[c]
1	Indole	C_6H_5I	8	96	(Huang et al., 2008)
2	Indole	p-$CH_3C_6H_4I$	10	90	(Veisi et al., 2017)
3	Indole	p-ClC_6H_4I	10	92	(Akhavan et al., 2018)
4	Indole	p-$OCH_3C_6H_4I$	10	92	(Islam et al., 2012)
5	Indole	p-$NO_2C_6H_4I$	8	96	(Akhavan et al., 2018)
6	Indole	o-$OCH_3C_6H_4I$	10	90	(Akhavan et al., 2018)
7	Aniline	C_6H_5I	3	96	(Kantam et al., 2008)
8	Aniline	p-$CH_3C_6H_4I$	3	92	(Islam et al., 2012)
9	Aniline	p-ClC_6H_4I	4	90	(Islam et al., 2012)
10	Aniline	p-$OCH_3C_6H_4I$	4	90	(Jammi et al., 1971)
11	Aniline	p-$NO_2C_6H_4I$	2	94	(Kantam et al., 2008)
12	Aniline	o-$OCH_3C_6H_4I$	2	85	(Rout et al., 2007)
13	Imidazole	C_6H_5I	10	90	(Islam et al., 2012)
14	Imidazole	p-$CH_3C_6H_4I$	10	80	(Zhu et al., 2007)
15	Imidazole	p-$OCH_3C_6H_4I$	10	70	(Islam et al., 2012)
16	Phenol	C_6H_5I	7	90	(Jogdand et al., 2009)
17	Phenol	p-$CH_3C_6H_4I$	8	88	(Jogdand et al., 2009)
18	Phenol	p-ClC_6H_4I	8	90	(Veisi et al., 2017)
19	Phenol	p-$OCH_3C_6H_4I$	8	90	(Rout et al., 2007)
20	Phenol	p-$NO_2C_6H_4I$	7	95	(Rout et al., 2007)
21	Phenol	o-$OCH_3C_6H_4I$	10	80	(Tao and Lei, 2007)
22	4-Methylphenol	C_6H_5I	10	80	(Ghorbani-Vaghei et al., 2013)
23	4-Methoxylphenol	C_6H_5I	8	96	(Veisi et al., 2017)
24	2-Methylphenol	C_6H_5I	12	85	(Veisi et al., 2017)

[a] Reaction conditions: amines/phenols (1.0 mmol), iodobenzene (1.1 mmol), CS-Cu NPs (0.2 mol%), KOH (1.5 mmol), DMSO (3.0 mL) were stirred for desired time under a nitrogen atmosphere at 100 °C; [b]Isolated yield; [c]Known product
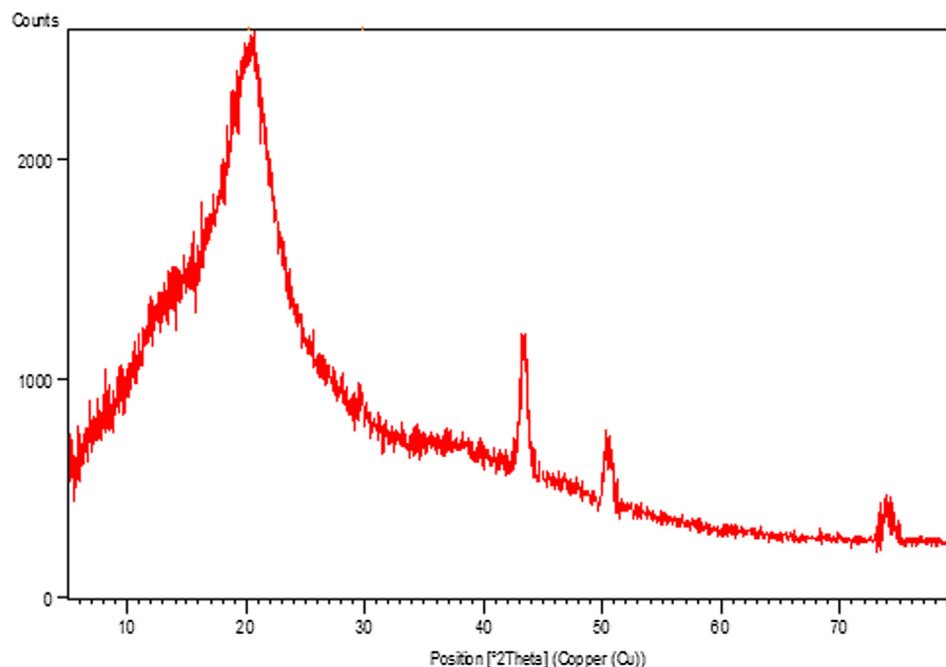
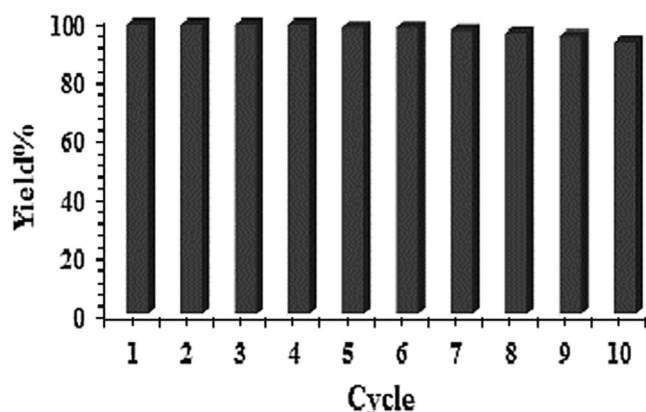**Fig. 5** XRD pattern of recycled catalyst after 10th run.

Fig. 4 Recycling of the catalyst for the reaction of indole with iodobenzene.

results, we believe, will definitely open up a wing towards anti-cancer research in future.

In the present study, the cytotoxicity of CS-Cu NPs was explored by studying its interaction with normal (HUVEC), UM-UC-3 (Transitional cell carcinoma), SCaBER (Squamous cell carcinoma), and TCCSUP (Grade IV, transitional cell carcinoma) cell lines by MTT assay for 48 h. The interactions being expressed as cell viability (%) was observed at different CS-Cu NPs concentrations (0–1000 μg/mL) with the four cell lines which have been shown in Fig. 6. In all the cases the % cell viability gets reduced with increasing nanocomposite con-

centrations. The IC_{50} values of CS-Cu NPs against UM-UC-3 (Transitional cell carcinoma), SCaBER (Squamous cell carcinoma), and TCCSUP (Grade IV, transitional cell carcinoma) cell lines were found 238, 404, and 569 μg/mL, respectively (Table 3). Thereby, the best cytotoxicity results and anti-human bladder cancer potentials of our nanocomposite was observed in the case of the PC-14 cell line.

The numbers indicate the percent of cell viability in the concentrations of 0–1000 μg/mL of nanocomposite against several human bladder cancer cell lines.

4. Conclusion

In summary, spherical shaped CS-Cu NPs nanocomposite with average mean sizes in the range of 10–20 nm and an *fcc* crystal structure were synthesized in a chitosan medium through a simple chemical method. The Cu NPs were characterized by FT-IR, FESEM-EDX, TEM, UV–Vis, and XRD analysis. Catalytic applications of the CS-Cu NPs nanocomposite were investigated in the C–N/C–O cross coupling reactions of aryl and heteroaryl nucleophiles with substituted aryl iodides. The designed protocol draws attention in terms of its simple, handy and cost-effective of nanocatalyst, convenient operations, reusability of catalyst and excellent yields. The CS-Cu NPs was also assessed in biological applications i.e. anticancer (adenocarcinoma) activities. It showed significant cytotoxic activities against common human bladder cancer cell lines i.e., UM-UC-3 (Transitional cell carcinoma), SCaBER (Squamous cell carcinoma), and TCCSUP (Grade IV, transitional cell carcinoma) cell lines.
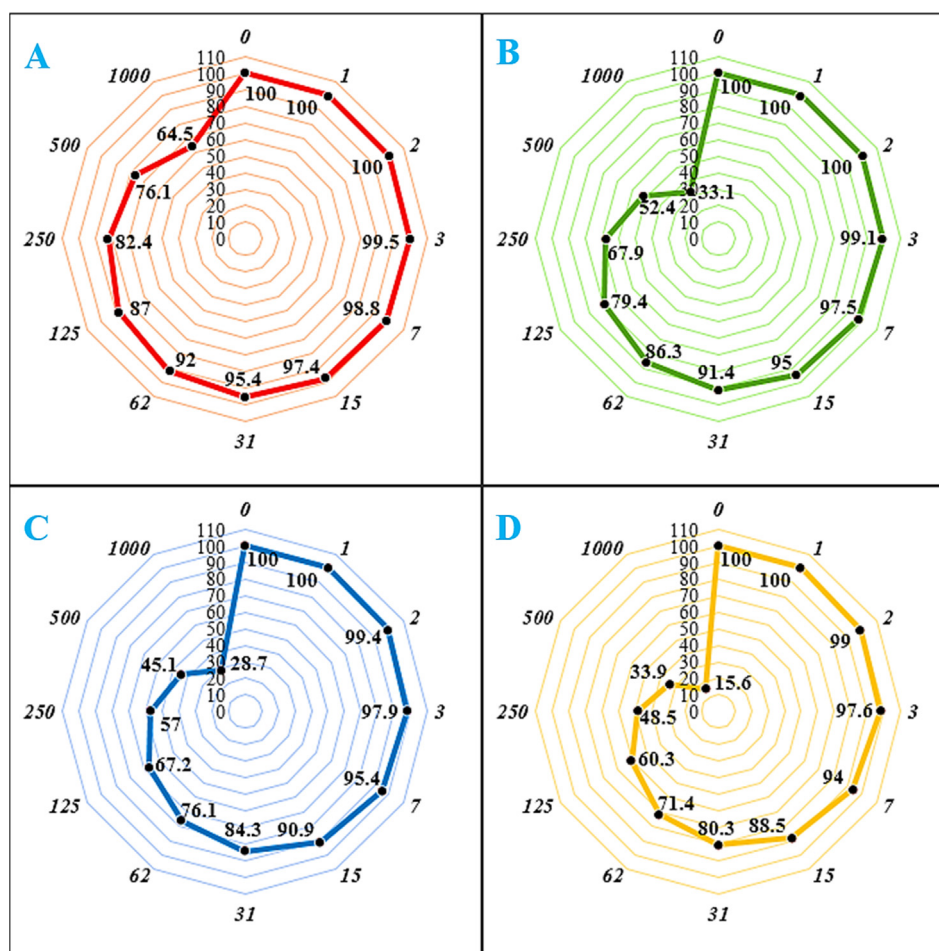
Fig. 6 The anti-human bladder cancer properties (Cell viability (%)) of CS-Cu NPs (Concentrations of 0–1000 µg/mL) against HUVEC (A), UM-UC-3 (Transitional cell carcinoma (A)), SCaBER (Squamous cell carcinoma (B)), and TCCSUP (Grade IV, transitional cell carcinoma (C)) cell lines.

Table 3 The IC50 of CS-Cu NPs in the anti-human bladder cancer test.

	HUVEC	UM-UC-3	SCaBER	TCCSUP
IC50 (µg/mL)	–	569	404	238

Declaration of Competing Interest

The authors declare that they have no known competing financial interests or personal relationships that could have appeared to influence the work reported in this paper.

Appendix A. Supplementary data

Supplementary data to this article can be found online at https://doi.org/10.1016/j.arabjc.2021.103259.

References

a) P. N. Craig, In Comprehensive Medicinal Chemistry; Drayton, C. J., Ed.; Pergamon Press: New York, 1991; Vol. 8; b) T. Wiglenda, R. J. Gust, Med. Chem. 2007, 50,1475.

Yoshikawa, S., Shinzawa-Itoh, K., Nakashima, R., Yaono, R., Yamashita, E., Inoue, N., Yao, M., Fei, M.J., Libeu, C.P., Mizushima, T., Yamaguchi, H., Tomizaki, T., Tsukihara, T., 1998. Science 280, 1723.

For reviews, see: a) V. Nair, S. Bindu, V. Sreekumar, Angew. Chem., Int. Ed. 2004,43,5130; b) W. A. Hermann, Angew. Chem. Int. Ed. 2002, 41, 1290.

Stabler, S.R., 1994. Synth. Commun. 24, 123.

Hartwig, J.F. in: Modern Amination Methods(Ed.: A. Ricci), Wiley–VCH, Weinheim, 2000, pp.195-262.

Hartwig, J.F., 1998. Angew. Chem. Int. Ed. 37, 2046–2067.

Rodriguez, J., Adet, N., Merceron, N.-S., Bourissou, D., 2020. Chem. Commun. 56, 94–97.

Akram, M.O., Das, A., Chakrabarty, I., Patil, N.T., 2019. Org. Lett. 21 (19), 8101–8105.

L. Capdevila, E. Andris, A. Briš, M. Tarrés, S. R.-Gómez, J. Roithová, X. Ribas, ACS Catal. 2018, 8, 11, 10430–10436.

Das, R., Mandal, M., Chakraborty, D., 2013. Asian J. Org. Chem. 2, 579–585.

Kuo, C.-H., Huang, M.H., 2010. Nano Today. 5, 106–116.

Zhang, Q., Zhang, K., Xu, D., Yang, G., Huang, H., Nie, F., Liu, C., Yang, S., 2014. Prog. Mater. Sci. 60, 208–337.

Xu, J., Li, X.M., Wu, X., Wang, W.Z., Fan, R., Liu, X.K., Xu, H.L., 2016. J. Phys. Chem. C 120, 12666–12672.

Ranu, B.C., Dey, R., Chatterjee, T., Ahammed, S., 2012. ChemSusChem 5, 22–44.

B. C. Ranu, D. Saha, D. Kundu and N. Mukherjee, in Nanocatalysis: Synthesis and Applications, ed. V. Polshettiwar and T. Asefa, John Wiley & Sons, Hoboken (NJ), 1st edn., 2013, ch. 6, pp. 189-220.

Sambiagio, C., Marsden, S.P., Blacker, A.J., McGowan, P.C., 2014. Chem. Soc. Rev. 43, 3525–3550.

Son, S.U., Park, I.K., Park, J., Hyeon, T., 2004. Chem. Commun., 778–779

Rout, L., Jammi, S., Punniyamurthy, T., 2007. Org. Lett. 9, 3397–3399.

Kidwai, M., Mishra, N.K., Bhardwaj, S., Jahan, A., Kumar, A., Mozumdar, S., 2010. ChemCatChem 2, 1312–1317.

Pai, G., Chattopadhyay, A.P., 2014. Tetrahedron Lett. 55, 941–944.

Reddy, P.L., Arundhathi, R., Rawat, D.S., 2015. RSC Adv. 5, 92121–92127.

Nador, F., Volpe, M.A., Alonso, F., Radivoy, G., 2014. Tetrahedron 70, 6082–6087.

Mitrofanov, A.Y., Murashkina, A.V., Martín-García, I., Alonso, F., Beletskaya, I.P., 2017. Catal. Sci. Technol. 7, 4401–4412.

Halder, M., Islam, M.M., Ansari, Z., Ahammed, S., Sen, K., Islam, S. M., 2017. ACS Sustainable Chem. Eng. 5, 648–657.

Makhubela, B.C.E., Jardine, A., Smith, G.S., 2011. Applied Catal A: Gen 393, 231–241.

Leonhardt, S.E.S., Stolle, A., Ondruschka, B., Cravotto, G., De Leo, C., Jandt, K.D., Keller, T.F., 2010. Appl. Catal. A: Gen. 379, 30–37.

Muzzarelli, R.A.A., 2011. Carbohyd. Polym. 84, 54–63.

Adlim, M., Abu Bakar, M., Liew, K.Y., Ismail, J., 2004. J. Mol. Catal. A-Chem. 212, 141–149.

Xu, T., Xin, M., Li, M., Huang, H., Zhou, S., 2010. Carbohyd. Polym. 81, 931–936.

Guinesi, L.S., Cavalheiro, É.T.G., 2006. Carbohyd. Polym. 65, 557–561.

Zhu, J., Wang, P.C., Lu, M., 2012. New J. Chem. 36, 2587–2592.

Baran, T., Menteş, A., Arslan, H., 2015. Int. J. Biol. Macromol. 72, 94–103.

Baran, T., Menteş, A., 2015. Int. J. Biol. Macromol. 79, 542–554.

Antony, R., David, S.T., Saravanan, K., Karuppasamy, K., Balakumar, S., 2013. Spectrochim. Acta. A. 103, 423–430.

(a) M. M. Zangeneh,S. Bovandi, S. Gharehyakheh,A. Zangeneh, P. Irani, Appl. Organometal. Chem. 33 (2019) e4961. (b) M. M. Zangeneh, Z. Joshani, A. Zangeneh, E. Miri, Appl. Organometal. Chem. 33 (2019) e5016. (c) A. R. Jalalvand, M. Zhaleh, S. Goorani, M. M. Zangeneh, N. Seydi, A. Zangeneh, R. Moradi, J. Photochem. Photobiol. B. 192 (2019) 103–112. (d) A. Zangeneh, M. M. Zangeneh, Appl. Organometal. Chem. 34 (2020) e5290. (h) M. M. Zangeneh, A. Zangeneh, Appl. Organometal. Chem. 34 (2020) e5271.

Mallick, S., Sharma, S., Banerjee, M., Ghosh, S.S., Chattopadhyay, A., et al, 2012. ACS Appl Mater Interfaces 4, 1313–1323.

Mallick, K., Witcomb, M.J., Scurrell, M.S., 2006. Eur Polym J 42, 670–675.

Zain, N.M., Stapley, A.G., Shama, G., 2014. Carbohydr Polym 112, 195–202.

Cardenas, T., Galo, S., Johana, I.M., Lucia, H., 2002. Bol. Soc. Chil. Quím. 47, 529–535.

Chen, D.H., Wu, S.H., 2000. Chem. Mater. 12, 1354–1360.

Dang, T.M.D., Le, T.T.T., 2011. Adv. Nat. Sci. Nanosci. Nanotechnol., 2 https://doi.org/10.1088/2043-6262/2/1/015009.

Raffi, M., Mehrwan, S., Bhatti, T.M., Akhter, J.I., Hameed, A., Yawar, W., Hasan, M.M., 2010. Ann. Microbiol. 60, 75–80.

Xie, Y.X., Pi, S.F., Wang, J., Yin, D.L., Li, J.H., 2006. J. Org. Chem. 71, 8324.

Huang, Y.Z., Gao, J., Ma, H., Miao, H., Xu, J., 2008. Tetrahedron Lett. 49, 948.

Kantam, M.L., Roy, R., Roy, S., Sreedhar, B., De, R.L., 2008. Catal. Commun. 9, 2226.

Islam, S.M., Mondal, S., Mondal, P., Singh Roy, S., Tuhin, K., Salam, N., Mobarak, M., 2012. J. Organomet. Chem. 696, 4264.

Tao, M., Lei, W., 2007. Tetrahedron Lett. 48, 95.

Jogdand, N.R., Shingate, B.B., Shingare, M.S., 2009. Tetrahedron Lett. 50, 4019.

Jammi, S., Sakthivel, S., Rout, L., Mukherjee, T., Mandal, S., Mitra, R., Saha, P., 1971. Punniyamurthy. T. J. Org. Chem. 2009, 74.

Rout, L., Sen, T.K., Punniyamurthy, T., 2007. Angew. Chem. Int. Ed. 46, 5583.

Veisi, H., Hamelian, M., Hemmati, S., Dalvand, A., 2017. Tetrahedrom Lett. 58, 4440.

Ghorbani-Vaghei, R., Hemmati, S., Veisi, H., 2013. Tetrahedron Lett. 54, 7095.

Zhu, J.B., Cheng, L., Zhang, Y., Xie, R.G., You, J.S., 2007. J. Org. Chem. 72, 2737.

Islam, SM; Mondal, S; Mondal, P; Singh Roy, S; Tuhin, K; Salam, N; Mobarak, M. J. Organomet. Chem. 2012, 696, 4264.

Veisi, H., Metghalchi, Y., Hekmati, M., Samadzadeh, S., 2017. Appl. Organomet. Chem. 31, 3676.

Akhavan, M., Hemmati, S., Hekmati, M., Veisi, H., 2018. New J. Chem. 42, 2782.